JM3 Journal of Micro/Nanopatterning, Materials, and Metrology

RESEARCH PAPER

Stabilizing high aspect ratio x-ray gratings with top layer resist grid

Michael Richter,[a] Thomas Beckenbach,[b] Constantin Rauch,[c] Stephan Schreiner,[c] Marcus Zuber,[d] Elias Hamann,[d] Arndt Last,[a] Martin Börner,[a] Jan Korvink,[a] and Pascal Meyer[a,*]

[a]Karlsruhe Institute for Technology (KIT), Institute for Microstructure, Eggenstein-Leopoldshafen, Germany
[b]Microworks GmbH, Karlsruhe, Germany
[c]Friedrich-Alexander-Universität Erlangen-Nürnberg, Erlangen Centre for Astroparticle Physics (ECAP), Erlangen, Germany
[d]Institute for Photon Science and Synchrotron Radiation (IPS), Karlsruhe Institute of Technology (KIT), Eggenstein-Leopoldshafen, Germany

ABSTRACT. A problem with high aspect ratio x-ray gratings, fabricated by the deep x-ray LIGA process, is the collapse of the metallic structure when the resist is removed. A unique method that consists of positioning perpendicular metal bridges on top of the grating (roof bridges) is described and tested as a solution. First, a theoretical study is carried out on the transmission loss of such grids as a function of the thickness, their spacing, their materials (gold or nickel), and the x-ray energy. Different processes with their own advantages and disadvantages are possible and described. To further satisfy the requirement of curved gratings, two processes are tested in detail: structuring the x-ray grating with a laser and planarization followed by restructuring a second resist layer. In both cases, a second electroplating step is performed. Finally, a grating with a 12 cm bending radius and stabilization is fabricated. To assess the quality of the grids, two complementary methods are used: scanning electron microscopy and angular x-ray transmission. The latter one is an innovatively developed measurement process specially dedicated to x-ray gratings. The results for the fabrication processes are discussed and rated. The stability provided by the roof bridges works as intended, although the overall quality of the grating is slightly reduced.

Keywords: angular x-ray transmission; Talbot–Lau interferometry; x-ray grating; x-ray LIGA

Paper 23079G received Oct. 17, 2023; revised Jan. 5, 2024; accepted Jan. 24, 2024; published Feb. 14, 2024.

1 Introduction

X-ray imaging based on phase-sensitive measurements and a dark field is of great interest, especially for clinical diagnostics[1] in which the current absorption-based techniques offer little information on the soft tissue. Newer techniques such as the most promising Talbot–Lau interferometry[2] are probed as a suitable alternative.[3–5] This grating-based phase-contrast technique enables the measurement of small refractive index changes in matter with micrometer spatial resolution.

To date, flat gratings produced by the x-ray LIthographie, Galvanik, Abformung (LIGA) process,[6–8] Bosch process,[9] or chemical etching[10] are used primarily in laboratory setups.

*Address all correspondence to Pascal Meyer, pascal.meyer@kit.edu

Often these setups require a large-scale coherent x-ray source. However, when space is limited, as is in most clinical setups, a non-coherent x-ray source such as a tube is much more desirable. This has one major disadvantage: a source grating (the so called G0) is needed close to the source to achieve partial coherence. With a cone source profile, this leads to partial shadowing. To overcome this problem, two general solutions exist: (1) bending the flat gratings and (2) producing a grating with the lamellae already inclined in any way toward the source's center point. Of these two approaches, we chose the first as being the most flexible and direct.[11]

However, when the source grating, with a resist that is still present, is placed only a few centimeters away from it, a loss in visibility and therefore a loss in image quality is observed after several months of use. This effect is attributed to the aging of the resist under irradiation.

This effect is illustrated in Fig. 1 by a comparison of a grid before and after use. The grid, with a periodicity of 2.4 μm, was used for ~6 months but in a discontinuous way. The grid, with a resist that was present, was located at 20 cm from the source (50 kVp, 15 W), uncooled. There is no denying that the quality deteriorated considerably. The irradiated area, a dark circular surface, is visible on Fig. 1(a′). A comparison of the scanning electron microscopy (SEM) picture [Figs. 1(a), 1(a′), 1(b), 1(b′), 1(c), 1(c′), 1(d), and 1(d′)] taken at the same position on the grid is presented before and after usage.

For this problem, one immediate question arises: why is the grating not used without the resist? In this case, no such degradation would be expected. Just removing the resist, partially or totally, is unfortunately not the solution, when confronted with higher aspect ratios needed for G0/G2 gratings (see Fig. 2). Small cracks, which cause very small periodicity shifts and are more or less always present, will widen and the periodicity will shift or, in the worst case, the lamellae may collapse completely. In either case, the grating becomes unusable or is destroyed.

The aim of this work is to find a way to produce high aspect ratio gratings without resist. In addition, the process has to include the possibility of curving the grating when it is placed near the source to avoid shadowing. A strategy to process such gratings, as future applications, is presented at the end of the paper.

The path for the stability of the grids that we are going to follow consists of connecting the top end of the lamellae to stabilize them (roof bridges); the bases are already fixed to the substrate. We accidentally discovered this possibility when a grid was electroplated too long (overplating) and the surface lamellae were connected to each other [see Figs. 3(a) and 3(b)]. When the resist was removed for inspection, the lamellae did not shift or deform. From that point, the goal is to develop a new process for manufacturing these connections in a much more defined way [see Fig. 3(c)]. Primarily, this means that there is less influence on the transmission. In a way, this can be seen as an orthogonally oriented low absorption "long lamellae grating design" on the top of the high x-ray absorption grating.

2 Grating Production

From the mentioned techniques to produce the 1D-grids, the deep-x-ray lithography process[6–8] is performed (see Fig. 4). In a first step, a wafer is coated with a negative epoxy-based photoresist such as SU-8.[12,13] Graphite is used as the wafer material as it has a very stable interfacial connection to the lamellae and no lift-off is expected to happen with resist removal and bending.[11] Afterward, a mask with the grids design is copied into the resist with coherent synchrotron radiation. The irradiation was performed at the microstructure laboratory at the Karlsruhe Research Accelerator (KARA, Karlsruhe, Germany). The resist is developed using propylene glycol methyl ether acetate (PGMEA), and then the structure is electroplated. For the metal applied, there is a limited choice as a high x-ray absorption is mandatory for any reasonable lamellae height. These are mainly gold, nickel, some nickel alloys (nickel-cobalt and nickel-iron), and possibly bismuth, for which research is underway. In our case, the gratings are always produced in gold to have the height of the lamellae as low and stable as possible. As a last optional step, the resist can be removed, partially or totally, with plasma etching. Typically, this is done for inspection of the gratings surface (partially removed) or for low height structures (totally removed).

The layout used is known as a "bridge" design. This design (see Fig. 2) is used for high aspect ratio gratings having a small period and high lamellae height. Due to numerous reasons during the process, gratings are exposed to stress and potentially subject to photoresist lamellae

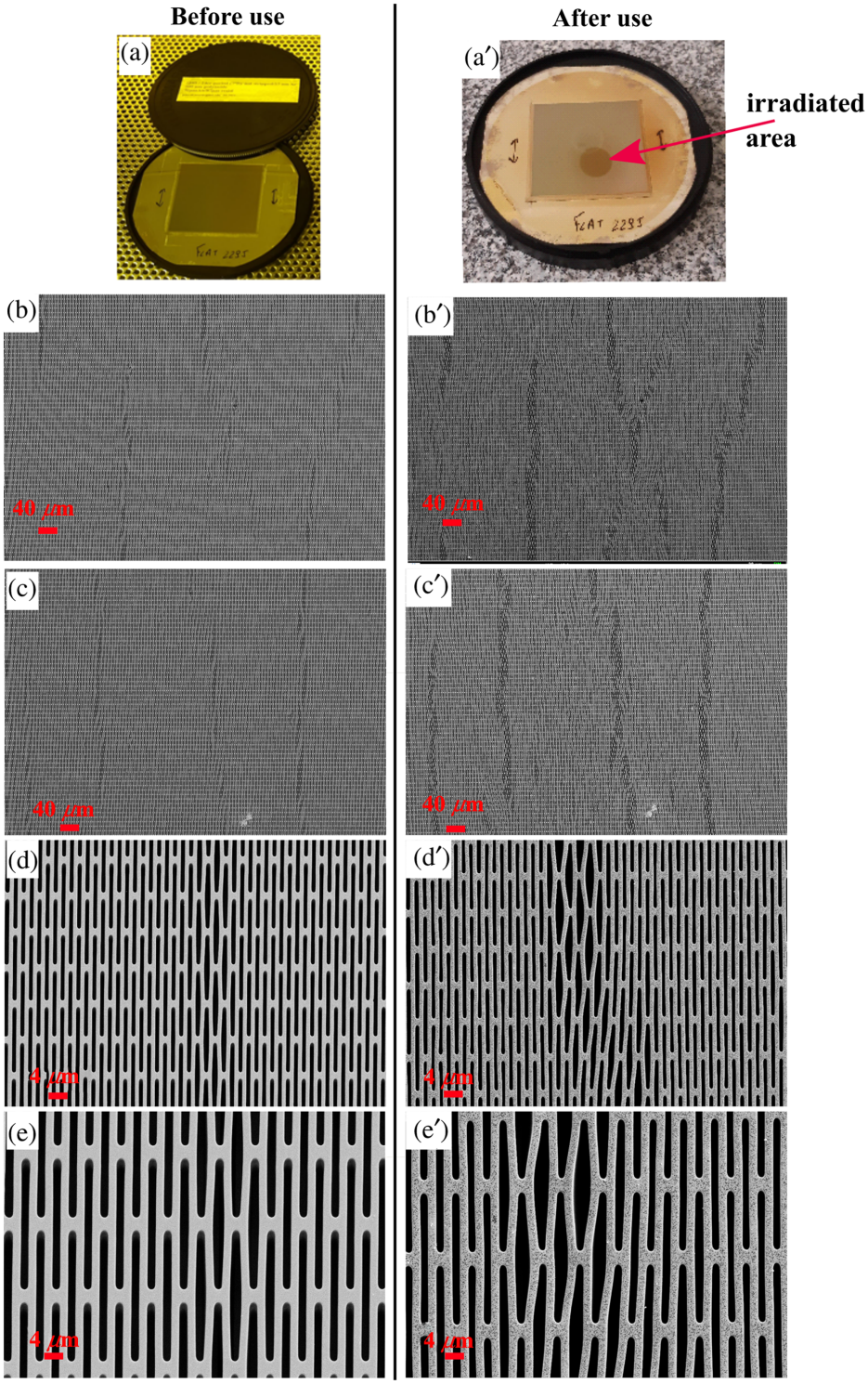

Fig. 1 Comparison of a 2.4 μm period grating before (a)–(e) and after (a')–(e') usage for ~6 months. A clear deterioration is visible.

deformation and cross-linking of the polymer. The solution consists of a small photoresist area (the bridge, typically 2 μm), connecting the photoresist lamellae for improved mechanical stability to avoid collapse during the subsequent electroplating step. Consequently, these regions are not electroplated and thus represent openings in the final grating, interrupting its metal lamellae.[14] In the following, the experiment concerns a 7.72 μm period grating with a duty cycle (DC; the ratio of the width of the absorber to the grating period) of 0.65. The grating area is

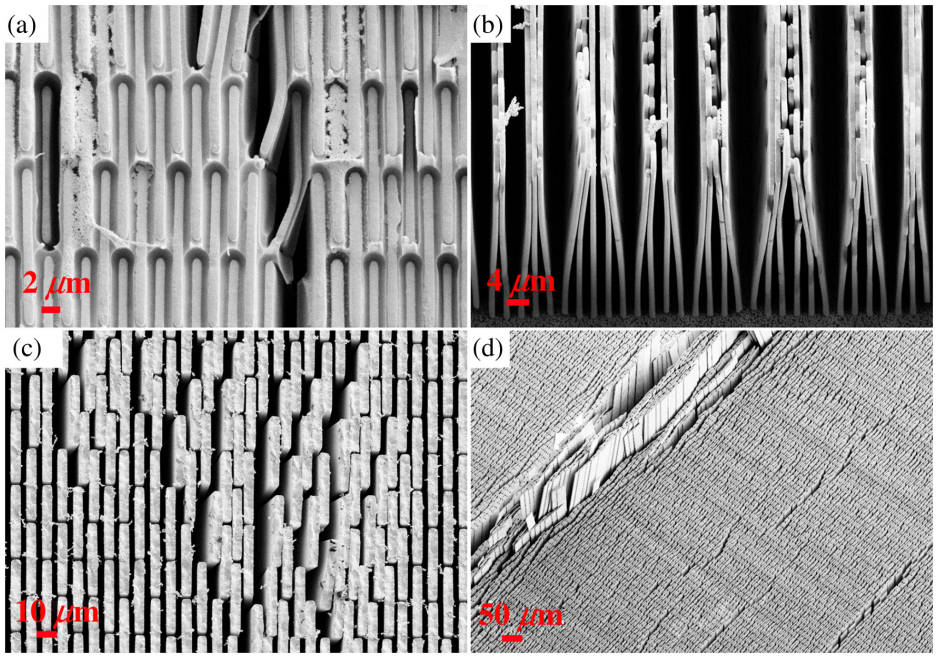

Fig. 2 SEM pictures of partially or totally stripped gratings. (a) A 2.4 μm period grating with a crack, (b) a totally collapsed 1.2 μm period grating, (c) a 4.8 μm period grating with widened period shifts, and (d) a 4.8 μm period grating with a large widened crack.

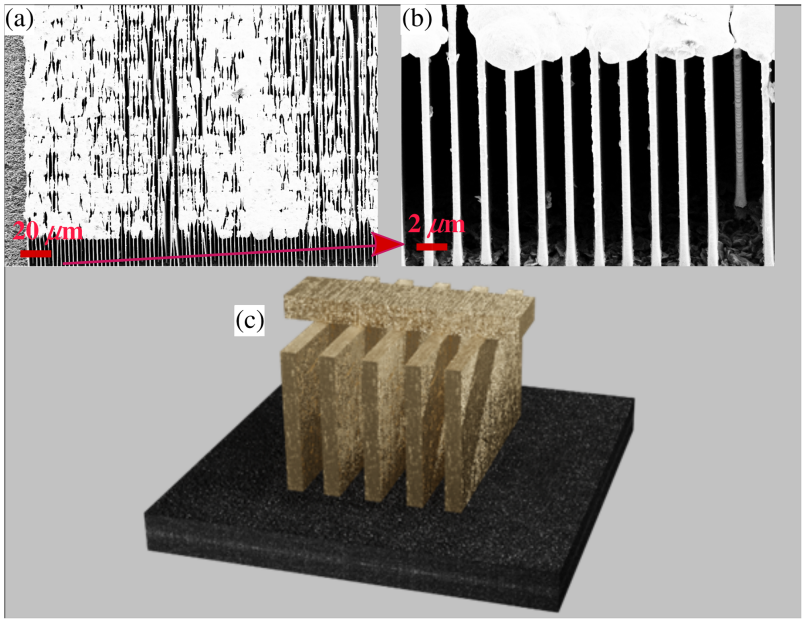

Fig. 3 Roof bridges. (a) and (b) Stripped lamellae connections accidentally obtained due to top overplating. (c) Ideal connection of the lamellae using a defined process.

2×2.5 cm. The substrate is a 500 μm thick graphite layer. The gold thickness of the gratings is in the range of 200 to 250 μm.

3 Gratings Quality and Parameter Characterization: SEM and Angular X-Ray Transmission

To characterize the gratings, we use two complementary methods:

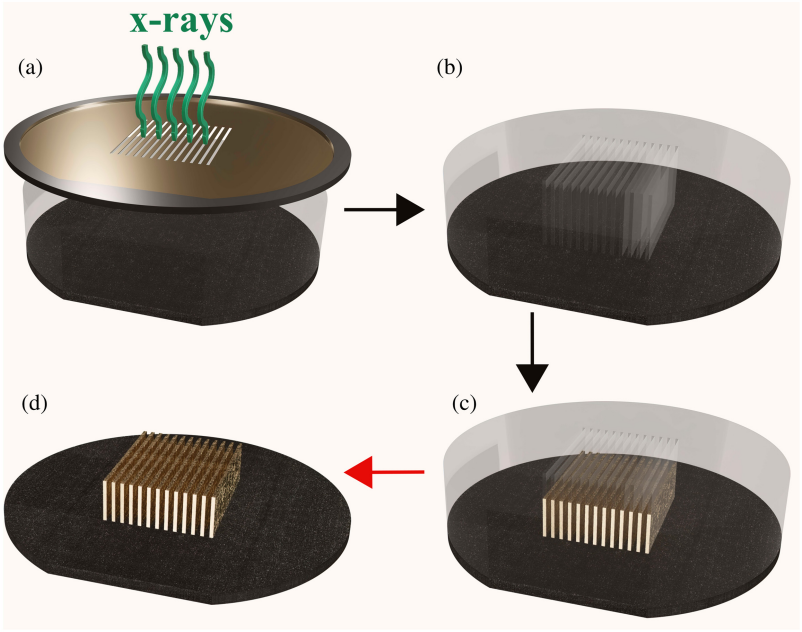

Fig. 4 X-ray LIGA process. (a) The wafer with resist is irradiated using synchrotron x-rays. (b) The resist layer is developed. (c) The structured resist is electroplated to form the metallic lamellae. (d) The resist can be removed.

- SEM: A Philips SEM Supra is used for measuring the period and DC and visualizing possible defects. The gratings surface is not 100% analyzed; a macro with point coordinates uniformly distributed over the grid surface is used. To date, this is the only standard method for characterizing the gratings before they are used. If the resist is not removed, the gratings are sputtered with silver, and only the resist picture is analyzed; no inside information on the metallic lamellae is available. To gain further information, the resist must be partially or totally removed. The information also only concerns the surface. To overcome these problems, a new technique is being developed: the angular x-ray transmission (AXT).[15,16]
- AXT: The AXT measurement technique is a non-destructive, macroscopic, spatially resolving quality and parameter control method for high aspect ratio x-ray absorption gratings. Based on AXT measurements (see Fig. 5), this technique should allow for determining the DC, the transmittance, the height, and the local inclination of the absorbing grating structures. The key advantage is a fast and extensive grating quality evaluation without the need for implementing an entire grating interferometer. However, one disadvantage lies in its novelty. No intensive studies on reproducibility, repeatability, or sensitivity have been carried out. Therefore, the measurement process is still very time consuming as every step involves several iterations of double-checking for consistency. This is the case for

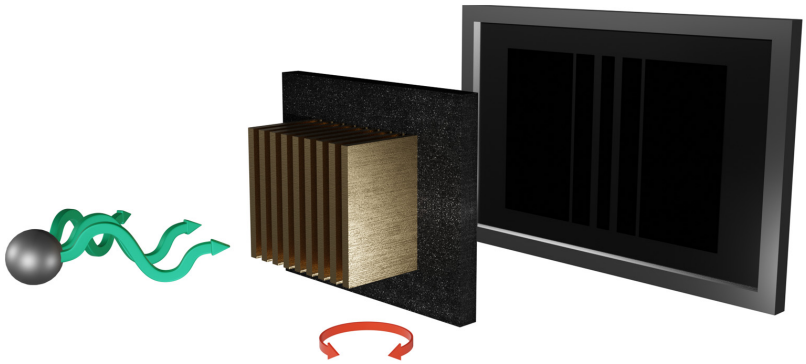

Fig. 5 AXT setup. The grating is aligned horizontally and vertically closes toward an x-ray tube source in the optical path. The grid is centered on the vertical axis of rotation.

mounting the grating as well as data acquisition and data analysis. In the following, the transmission and absorber inclination are studied. Each pixel (angle versus transmission) is fitted using a triangular fit; the transmission and deviation of the angle of the structures in relation to the theoretical angle are calculated. All of the experiments were carried out in the computed tomography laboratory (CT Lab) of the Institute for Photon Science and Synchrotron Radiation (IPS) at Karlsruhe Institute of Technology. An XWT-225-SE x-ray tube (X-RAY WorX, Garbsen, Germany) was operated using different voltages (30 to 120 kVp) and a power tungsten target of 15 W. As detector, a Perkin Elmer XRD 1621 flat panel (Gadox scintillator, 200×200 μm pixel size, 400×400 mm active area) is used. The gratings are fixed in a holder, which is attached to a multi-axis manipulator system. Unfortunately, due to practical reasons, it was not possible to perform all necessary experiments for all gratings involved. To extract/calculate the information, one code in Python and one for Matlab were developed.

4 Simulation

To estimate the influence of the roof bridges, a simulation study was performed to evaluate the loss of performance in terms of transmission as a function of material (gold or nickel), width of the roof bridges, and the space between them. In parallel, using the simulation results, we explore different solutions to realize these connections. For the different tests, the same design is used, namely a 7.72 μm period gratings with bridge design with a DC of about 0.65 and dimensions of 2×2 cm.

To characterize the transmission performance first, a figure of merit for two materials, gold and nickel, is given (see Fig. 6). The transmission of the roof bridges must be as high as possible. The thickness is calculated as a function of the covered area ratio of the gratings and energy for a

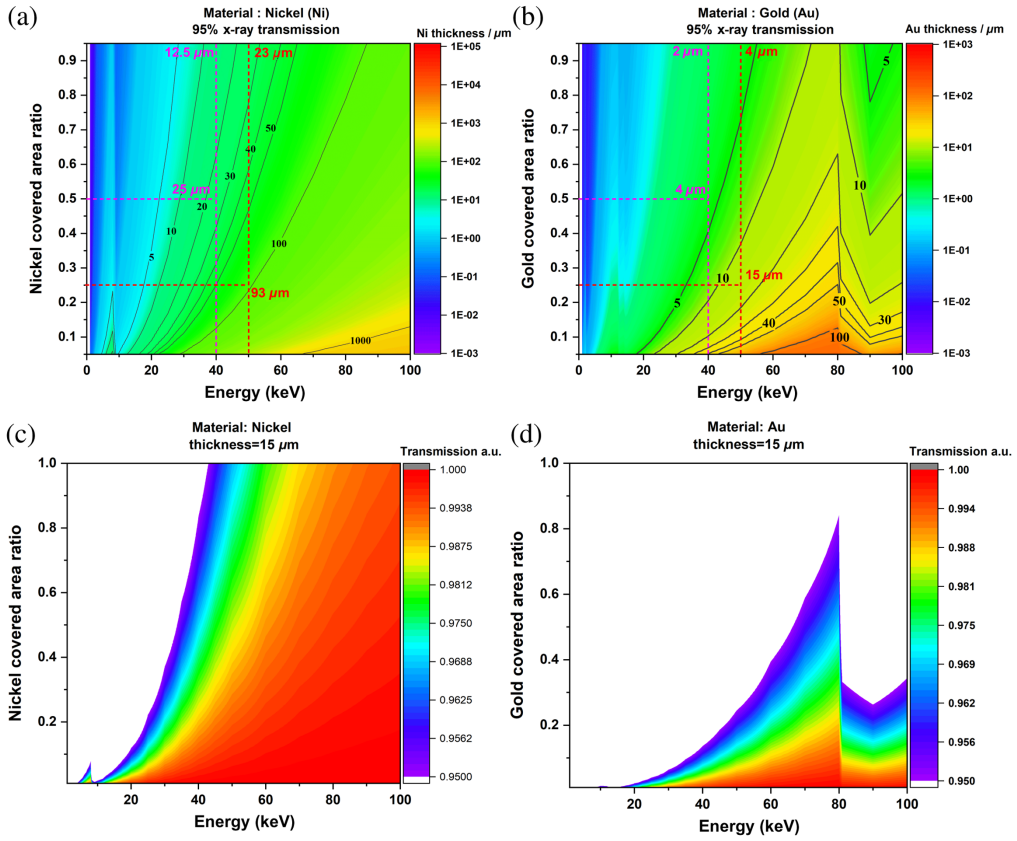

Fig. 6 X-ray transmission performance figure of merit for two materials, gold and nickel. (a) and (b) Thickness calculated as a function of the covered area ratio of the gratings and energy for a 95% transmission. (c) and (d) Minimum 95% transmission calculated as a function of energy and covered area ratio of the gratings for a thickness of 15 μm.

goal of a minimum 95% transmission. The minimum 95% transmission is also calculated as a function of energy and covered area ratio, using a thickness of 15 μm as an example. The metal covered area ratio is defined as the metal area divided by the grating area. A ratio of 1 indicates that the metal layer covers the whole grating, effectively corresponding to a single roof bridge with an infinite width. Comparatively, a ratio of 0.25 indicates roof bridges with widths of 4 μm, spaces of 16 μm, and a higher thickness depending on the energy.

From this study, the following facts emerge: nickel should be preferred, which in itself is not a discovery. As an example, for an energy of 50 keV and a ratio of 0.25 [see the Figs. 6(a) and 6(b)], the maximum thickness of nickel can be significant, 93 μm, compared with the 15 μm thickness of gold. Based on these results, an expectation for the AXT measurements is simulated using real grid geometries. The simulations were carried out using the Monte Carlo computer code Penelope.[17,18] In the following, two different geometries are used as base gratings: a 4.8 μm period and a 7.72 μm period, with a DC of 0.5 and 0.65, respectively. The geometry designs are presented in Figs. 7 and 8. Different roof designs with varying coverage ratios are tested for both gold and nickel as materials. The simulations cover two principle scenarios: a scenario in which the grating is used exactly as it is after the electroplating (the height being constant) and a scenario in which the height is lowered corresponding to any process that involves further

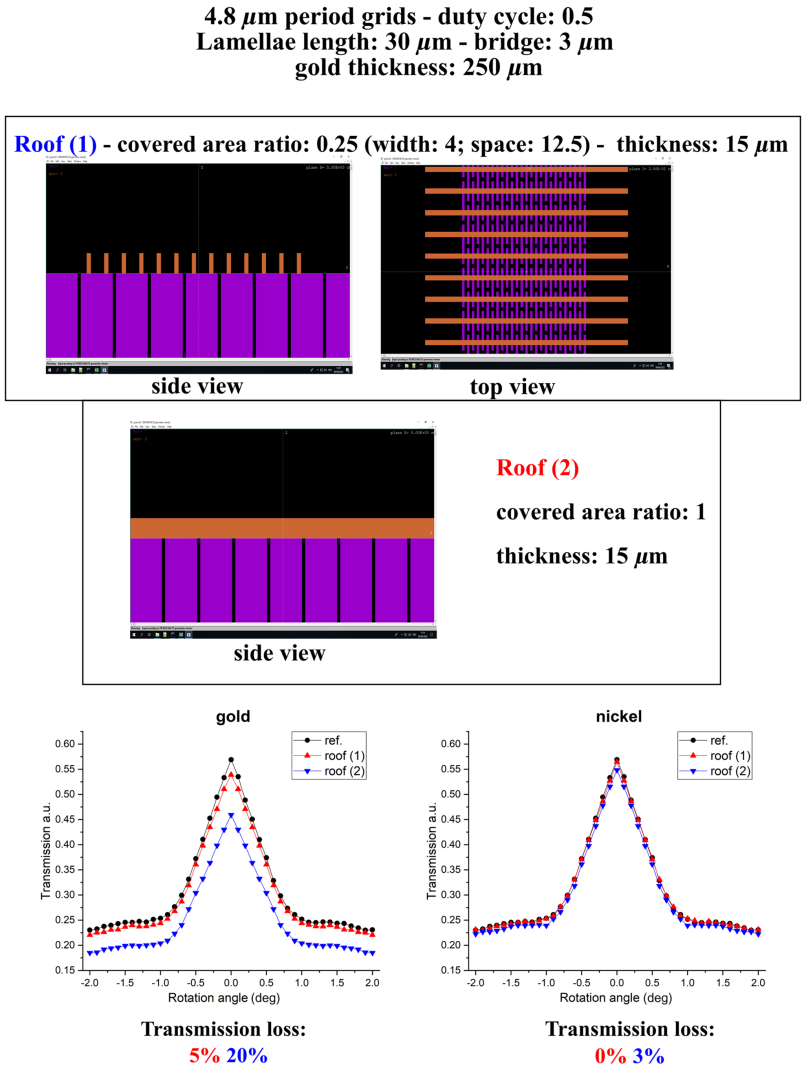

Fig. 7 AXT simulation concerning a 4.8 μm period grating (DC: 0.5; gold thickness: 250 μm; x-ray energy: 50 keV; cone beam; distance source-grating: 30 cm; distance grating-detector: 50 cm; pixel size: 200 μm) for two materials, gold and nickel, and two types of roof bridges [roof (1) and roof (2)].

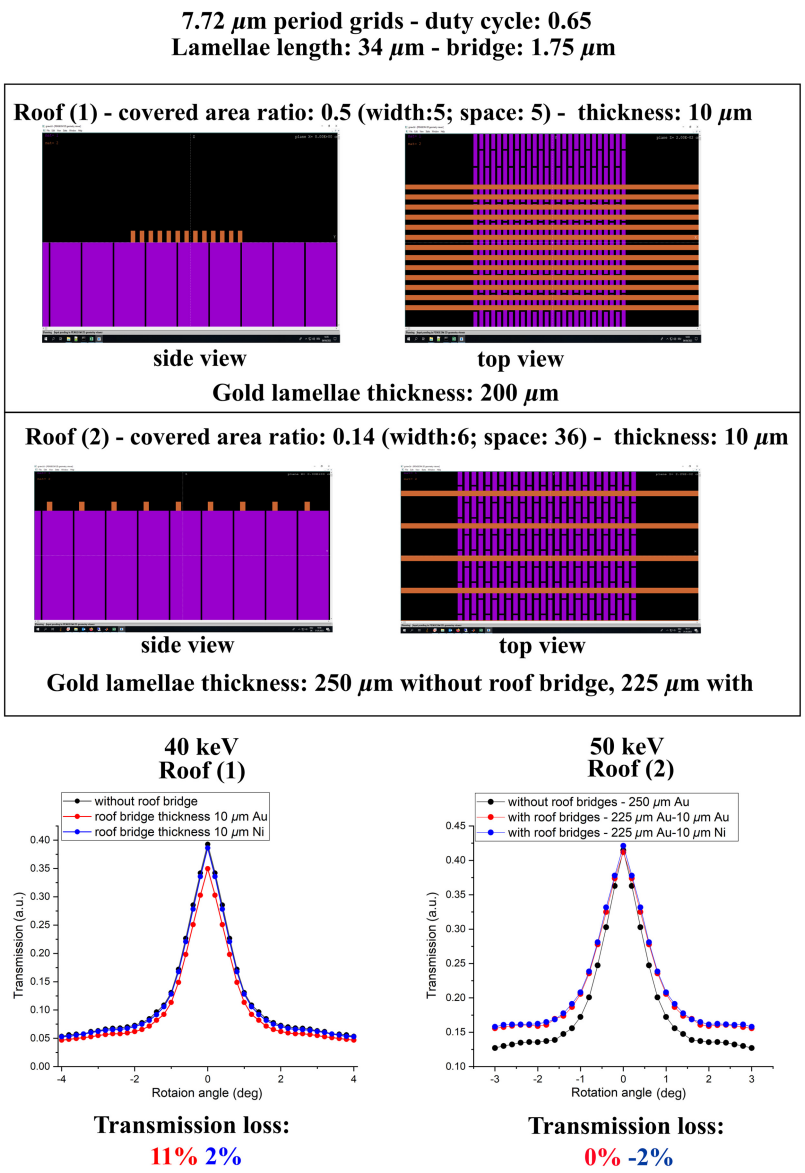

Fig. 8 AXT simulation concerning: (1) 7.72 μm period grating (DC: 0.65; gold thickness: 200 μm; x-ray energy: 40 keV; cone beam; distance source-grating: 30 cm; distance grating-detector: 120 cm; pixel size: 200 μm) for two materials, gold and nickel, and one type of roof bridge. (2) 7.72 μm period grating (DC: 0.65; gold thickness: 250 μm without roof bridges, 225 μm with roof bridges; x-ray energy: 50 keV; cone beam; distance source-grating: 30 cm; distance grating-detector: 120 cm; pixel size: 200 μm) for two materials, gold and nickel, and one type of roof bridge.

machining. All simulations, except for the one shown in Fig. 8, correspond to the first scenario. In this case, the AXT curves with the roof brides are below the ones without. In the case of scenario two, the curves with roof bridges could be over the ones without. The values obtained are in perfect agreement with those of the figures of merit and emphasize our roof bridges as a good stabilization solution.

4.1 State of the Art: Grating After the Electroplating Process

As mentioned, the stabilization concept involves fabricating a secondary structure on top of the grating. The process takes place after the LIGA electroplating step [see Fig. 4(c)]. Here, it is necessary to give a short overview of the state of the grating at this point as this highly influences the fabrication process. By producing high aspect ratio gratings, typically a resist layer with a thickness 20% to 30% higher than the desired gold height is used. This prevents the described overplating. Note that even by fully utilizing pulsed plating, the electroplating rate is

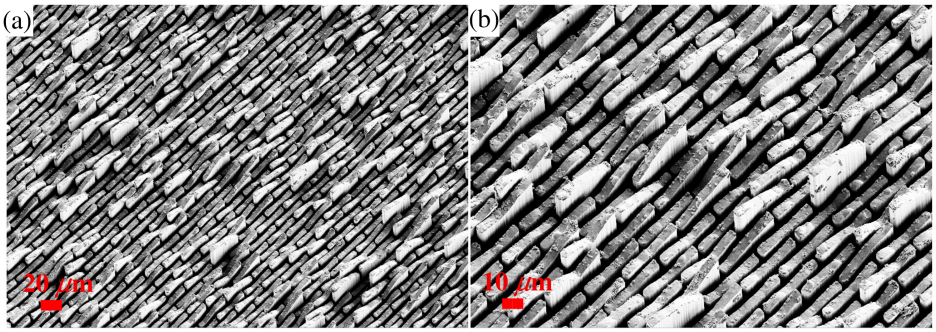

Fig. 9 7.72 μm grating with DC 0.6; the gold height is about 250 μm. SEM pictures after partially removing the resist (a) overview and b) details. The locally gold lamellae height variation is clearly visible.

not homogeneous over the whole surface and varies locally (see Fig. 9). This effect leads to height variations that are typically on the order of 10 μm and more.

4.2 Stabilization Methods: The Different Solutions

Taking into account the characteristics of the grids after the electroplating, as well as the thickness of the metal to be used for the roof bridges, so as not to significantly alter the transmission, three possible production paths can be identified (see Fig. 10):

- The grating is overplated. This could be realized using the same metal (gold) or moving to a less x-ray attenuating one, such as nickel. A planarization step follows to obtain the desired thickness.
- Grooves is structured in the overhead resist, down to the surface of the gold lamellae. This is realized with high precision laser cutting. A second electroplating step then takes place to fill the grooves.
- A planarization step first takes place, followed by the deposition of a thinner, more defined resist layer that is structured. Again, an additional electroplating step follows.

To further explore these solutions, a strengths, weaknesses, opportunities, and threats (SWOT) analysis of the appropriate options is presented in Table 1. The available method, the manufacturing time and the possibility or impossibility of obtaining bent gratings (see Table 1).

The easiest way seems to be the full covering of the grating. However, this method has a serious drawback: no suitable way was found to apply this fabrication path to a bent grating. Therefore, this method was not further considered in this study. For the remaining possibilities, the weaknesses and opportunities were comparable, and both processes were tested.

4.3 Laser Fabricated Roof Bridges

By directly structuring the excess resist with a high precision laser, a roof bridge pattern is fabricated [see Fig. 11(a)]. The laser used is an excimer argon fluoride laser (ArF laser): ATLEX-1000-I from ATL Lasertechnik GmbH. With 10 μm being the minimal possible width for the setup, this value was chosen for the cuts. The walls for the cuts produced this way show an almost optimal angle of nearly 90 deg toward the surface of the lamellae [see Fig. 11(b)]. Unfortunately, with this system, there is no option to cut more than one line at a time, and regular cooling periods need to be considered. To pattern a 10×6 mm area, about one day is needed, including cooling times. In total, this corresponds to a week for an area of 20×20 mm. A second existing KrF laser system, which has the option of multiple simultaneous cuts, unfortunately did not produce a usable wall angle deep enough into the surface and could not be used.

To estimate the needed depth of the laser cuts, the height of the lamellae is estimated using the electroplating deposition parameters. This and the resist height are then used for the depth of the laser cuts [see Fig. 11(a)]. As can be seen by the seemingly wider gaps [horizontal black space Fig. 11(b)], the height of the lamellae is not homogeneous over the entire grating area. Unfortunately, this leads to a major problem with this method: the height variations during

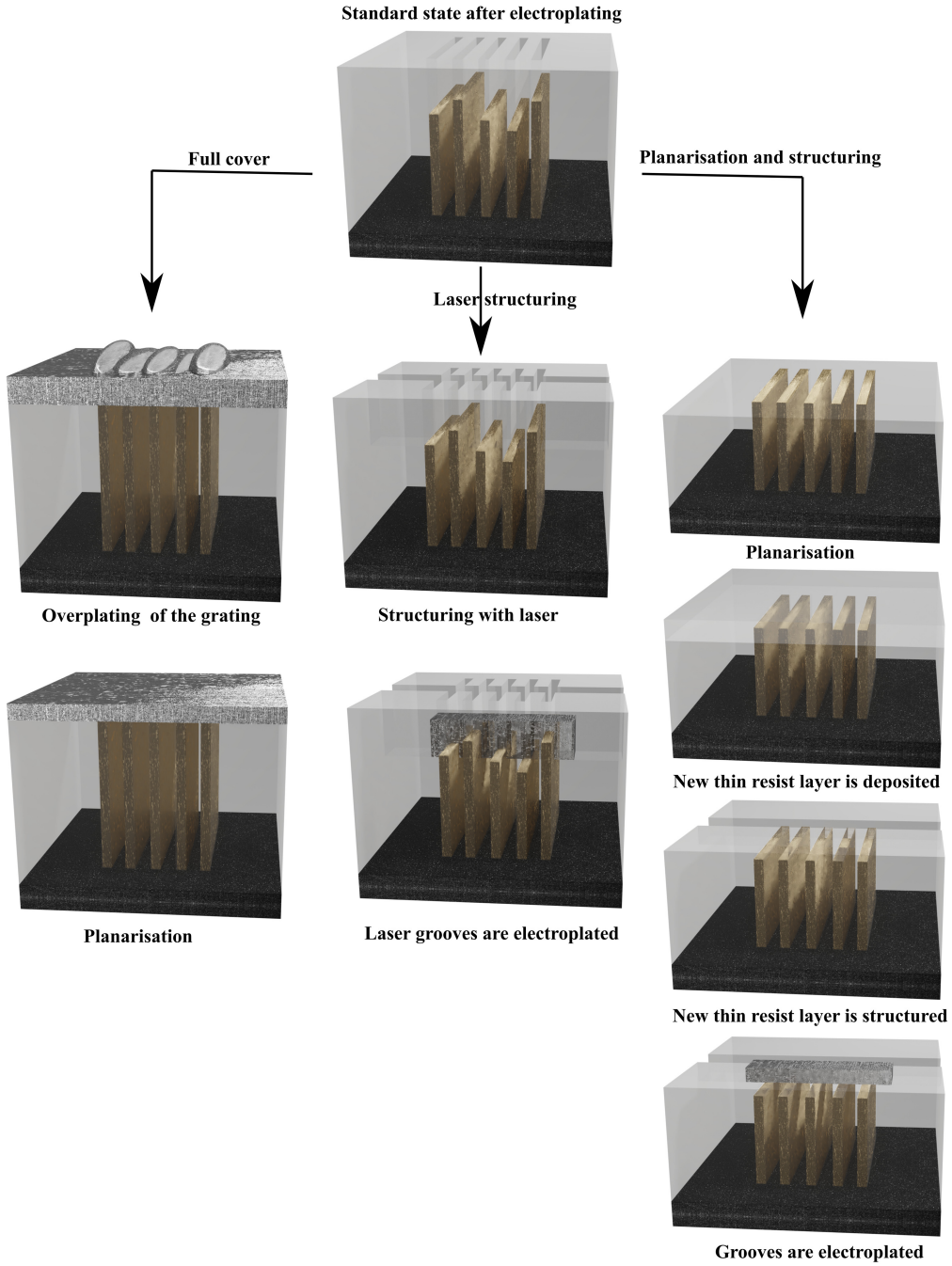

Fig. 10 Possible production paths for roof stabilized gratings: (left) overplating and planarization, (middle) laser cutting, and (right) planarization with secondary layering.

electroplating result in drastic differences in local growth rates. Consequently, the roof bridges become too inhomogeneous from an optical point of view [see Figs. 12(a) and 12(b)].

Without removing the resist, the AXT measurements concerning x-ray transmission (see Fig. 13) confirm the SEM analysis: the area with roof bridges has the expected significant reduction in transmission (20%) and enlarged transmission peak due to inhomogeneous height. The lamellae inclination angles are comparable; the shape of the curves is similar. After removing the resist, the curves widen, and the peaks are not sharp anymore. In the area with roof bridges, the inclination is still better. Stabilization is clearly present, but unfortunately, it is not in a desired or usable state. The process is very time consuming, and the result does not provide a quality that is suitable for any application. Therefore, it was not considered further.

Table 1 SWOT analysis for potential roof stabilization fabrication paths.

	(1) Overplating → planarization	(2) Structuring → electroplating	(3) Planarization → resist deposition → structuring → electroplating
Strength	• Straight forward • Different procedures possible: lapping/polishing, diamond turning, and diamond fly cutting	• Minor stress induced	• Best parameters control
Weakness	• Low thickness needed • No application for bent gratings	• Long fabrication time	• Very long fabrication time
Opportunity	• Only one more fabrication step needed after electroplating	• Less surface area, more thickness • Inspection possible	• Less surface area, more thickness • Inspection possible • Full control of all parameters for stabilization
Threat	• Due to inhomogeneous heights, not all lamellae may be connected	• Inhomogeneous growing of the roof bridges • Possibility of new product failure	• High-risk process • Possibility of new product failure

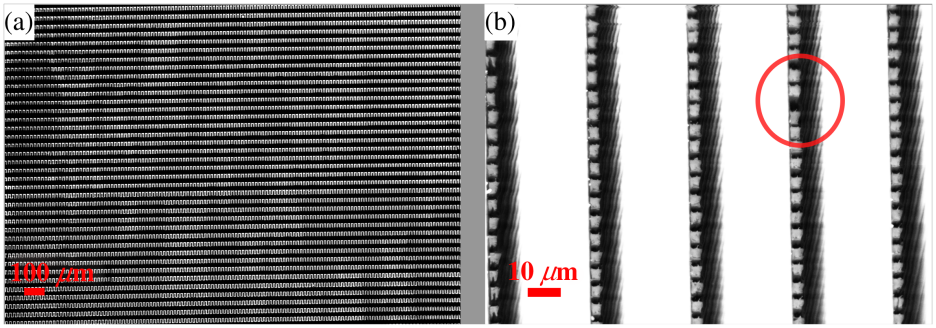

Fig. 11 Laser cuts in the excess resist. SEM pictures: (a) overall area as an overview of the homogeneity of structure and (b) close-up view into the deep cuts to inspect that the top ends of the lamellae are opened. Locally wider black space between the lamellae (red cycle) shows higher lamellae.

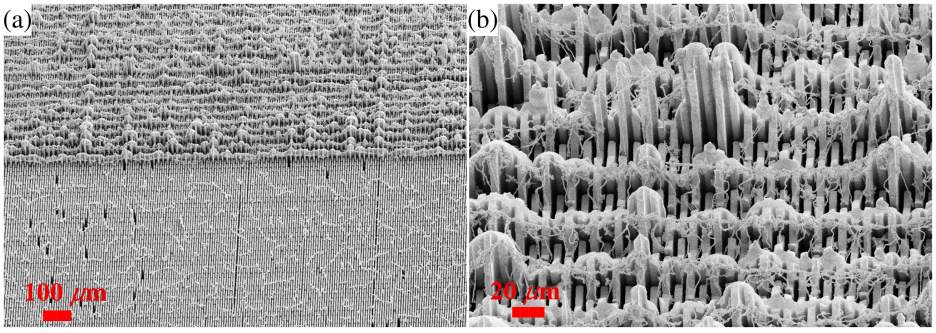

Fig. 12 Roof bridges as a result of laser cutting. SEM pictures: (a) overview and (b) details. Locally, the bridges are massively overgrown while being barely connected in other areas. Overall, the homogeneity is very bad.

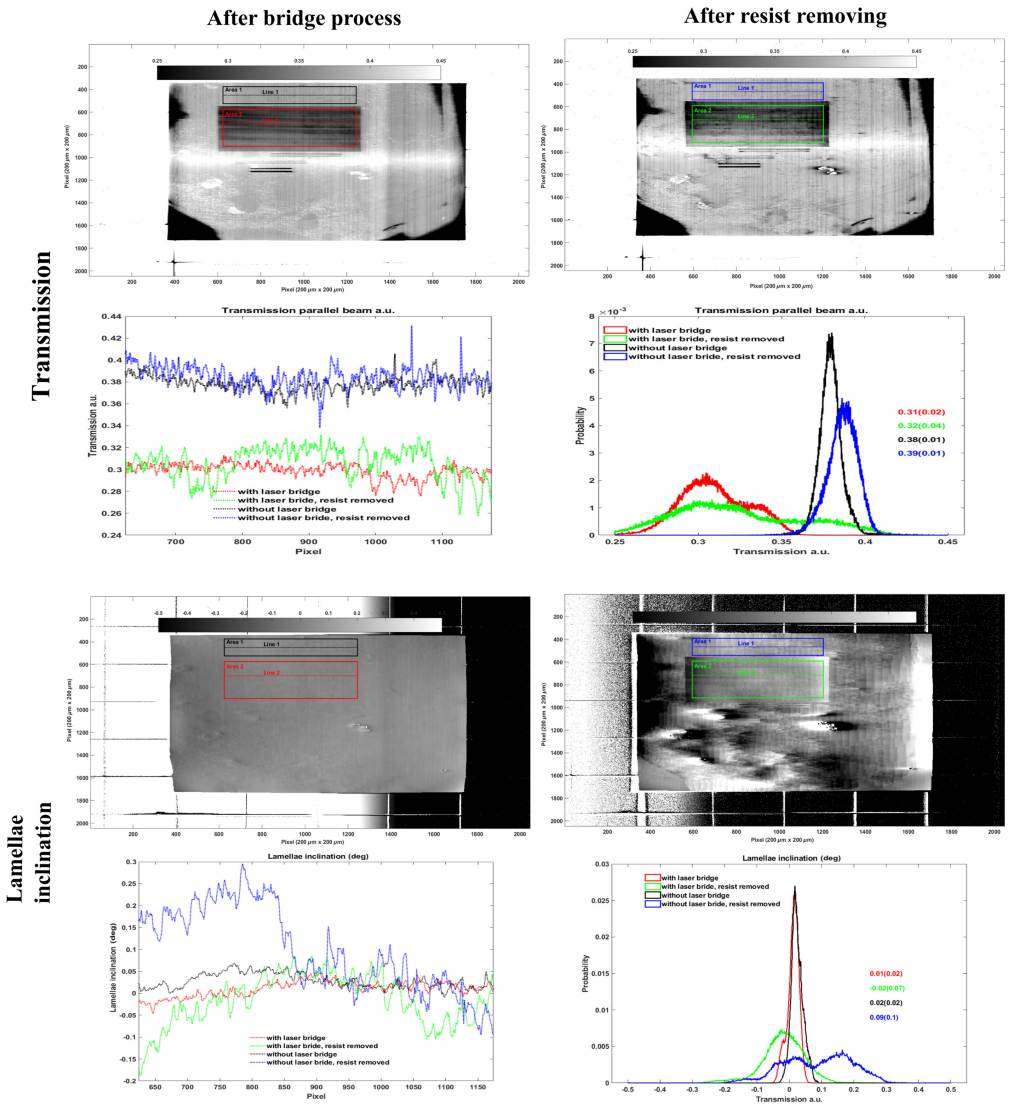

Fig. 13 AXT measurement results (transmission and lamellae inclination angle) after processing the roof bridges without and with removing the resist. An area and a profile in a part of the grating with roof bridges (line2, area2) and without roof bridges (line1, area1) are used for comparison.

4.4 Mechanical Surface Treatment

As the metal lamellae inhomogeneous height clearly is the problem, the only solution is to eliminate the height differences. A mechanical treatment of the surface (diamond fly cutting, diamond turning,[19,20] and lapping) is at first glance the least desired way due to the high risk of breaking and deforming the grating.

To achieve a homogeneous surface height and avoid the need for mechanical processing, a combination of very short resist stripping time with careful chemical gold etching to smooth out the surface can be performed as an alternative. However, this requires very thin layers to be removed one after the other and would take an impractical long time. Therefore, this was ruled out as the general production path. However, this process is still the optimal process for cleaning out the surface after a mechanical surface treatment.

It turned out that a mechanical processing of the surface is feasible and results in the desired surface homogeneity without too much disturbing the homogeneity of the grating.

4.4.1 *Diamond fly cutting*

For practical reasons, namely machine availability, the method chosen to remove the inhomogeneous surface is diamond fly cutting. The process is performed on a micromilling center

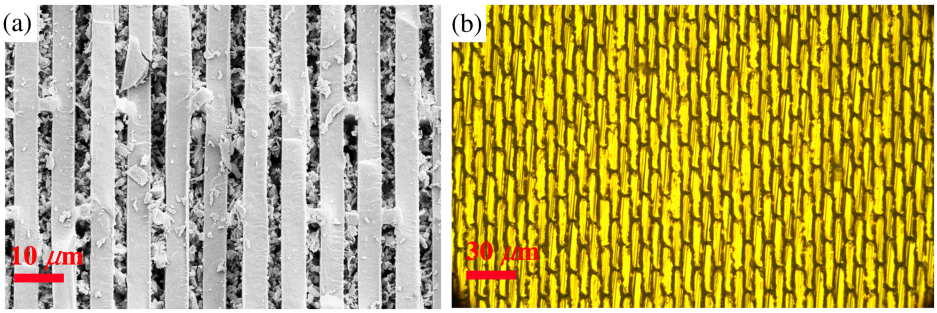

Fig. 14 (a) SEM picture: diamond turned resist surface. The underlying structure is well intact. (b) Optical picture: gold surface after full grinding process. The grating structure is well preserved.

hydrostatic series machines (LT Ultra MMC 600 2 Z, LT Ultra-Precision Technology GmbH, Germany). The wafer is positioned on a vacuum chuck, and the following parameters are used: 3000 rot./min with a Z step of 0.1 μm. The distortion introduced solely in the resist layer was found to be negligible [see Fig. 14(a)] (SEM picture). The grating structures underneath are preserved almost perfectly [see Fig. 14(b)] (optical picture). Only minor smearing of the metal is observed toward the edges of the individual lamellae.

In addition, the handling of the process is very convenient as it is very easy to see whether the gold surface in general is reached as the difference is either a shiny area or a dull gray one easily visible to the naked eye. Therefore, the loss in height can be kept at a minimum. The downside of this method, however, is its slow processing time of typically a week due to the careful and small Z steps. However, this cannot be avoided when an undisturbed surface is critical.

5 Top Bridges

After the surface machining, a second negative resist layer is spin coated on top of the grating. A thickness of 20 μm is always chosen to obtain a maximum stabilization height of 15 μm. To be sure that the lamellae gaps of around 2 μm are fully closed, at least around 6 μm in height is needed. In this second layer, an edge effect in the outer 1 mm is always present in the form of a height increase of an additional 10 μm around the edges of the gratings metal area. This effect is attributed, on the one hand, to an inhomogeneous heat distribution when the resist is dried as the thermal conductivity of the metal is much larger than the surrounding resist material and, on the other hand, to boundary effect during resist coating.

For creating the stabilization molds in the resist, two principal methods can be applied: direct laser writing (DLW, Heidelberg Instruments DLW66 fs) or a second LIGA process, which can be UV or x-ray. Neither is strictly better than the other, but each offers an advantage depending on what is being sought (see Table 2).

Both production paths were tested. Direct laser written roof bridges were tested for two independent gratings. A second LIGA step, using x-ray lithography, was included in the production of a bent grating with roof stabilization.

For the laser produced roof bridges, the edge effect is a problem as the laser cannot write the molds in this area down to the surface. Therefore, an outer layer of around 1 mm always has no

Table 2 Roof bridge production path comparison.

	DLW	2nd LIGA (UV or x-ray)
Strength	• Width and space of the roof bridges (very variable)	• Has no problems with edge effects • Production speed independent of the area
Weakness	• Problems with edge effects (the writing laser cannot focus to the bottom within the higher resist edges)	• A new mask needed for every parameter set or denser covering (parameters are not as freely chosen)

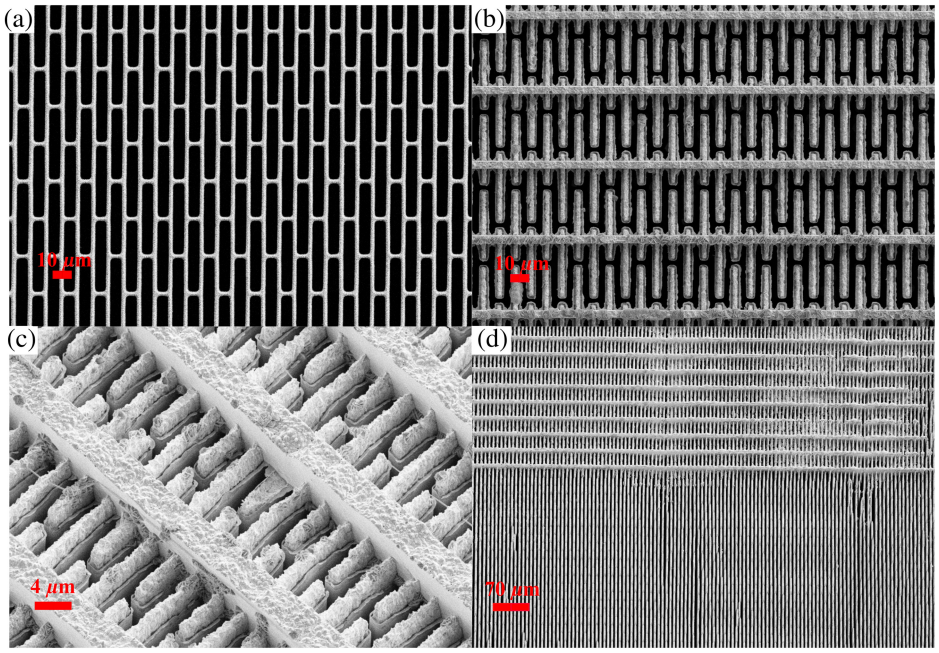

Fig. 15 Grating 1: SEM pictures. (a) Structure after electroplating. Only the resist structure is visible. (b) and (c) Roof bridges after removing the resist. (d) Area with roof bridges versus area without roof bridges after removing the resist.

stabilization. In the stabilized area, roof bridges with widths of 6 μm were produced. The spacing of the roof bridges was chosen at 36.5 μm, which corresponds to the distance between the resist bridges to minimize the roof bridged total area. The material chosen for the roof bridges here was gold, the same metal as the lamellae.

Concerning grating 1, the full area, except for the small outer ring, is covered with roof bridges. The lower part of grid 2 has a surface that was not intentionally stabilized, for comparison. Both gratings show a significantly improved quality over the previous laser cut grating. Inspection with SEM already displays roof bridges with a very defined width and height in the desired parameter range with total variations being less than 1 μm [see Figs. 15(b)–15(d) and Figs. 16(a), 16(b), and 16(d)].

The roof bridges connect a flat homogeneous surface. Compared with areas without bridges, the ones with bridges are of much better quality [see Fig. 15(d) versus Fig. 16(c)], and an improved status is expected regarding the AXT measurements. The roof bridges have a significantly improved quality compared with the laser cut roof bridges. The width and height are well defined, and the underlying lamellae grid is optically undisturbed.

The AXT measurements, however, only partially support the SEM analysis (see Figs. 17 and 18). The transmittance of the newly fabricated, stabilized gratings is significantly better than the one for laser cut roof bridges; the final transmittance is reduced by around 5%, which still matches the intended goal (see transmittance in Fig. 19). A degradation of the grating is unfortunately visible and preexisting defects in the grating worsen slightly as well.

The inclination variation widens in both gratings but stays qualitatively comparable to the initial grating. When the resist is removed, the inclination variation of the stabilized area only widens slightly more but stays almost the same in magnitude. The area that was not stabilized shows significant worsening of defects and presents a much more reduced quality of inclination stability (see the green curve in Fig. 18).

In both cases, the AXT measurements show that the gratings are clearly stabilized when the resist is removed, although the final grating quality is reduced.

5.1 Bent Stabilized Grating

In the case of LIGA processing, the larger height of the second resist layer around the edges is of no concern. The downside, however, is that a mask is needed. As stated, the best production

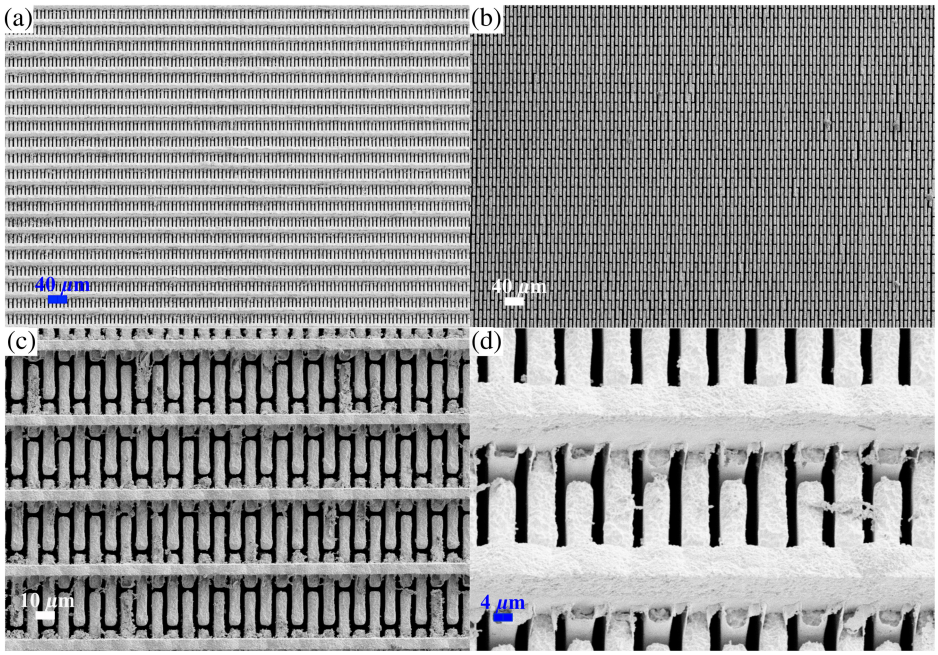

Fig. 16 Grating 2: SEM pictures. (a), (c), and (d) Roof bridges after removing the resist. (b) Area without roof bridges after removing the resist.

outcome is a minimal coverage from the roof bridges. This means that ideally every lamella is connected only once; *de facto* and a separate LIGA mask for every grating layout would be needed. For a proof of concept, a preexisting mask that has a period of 10 μm, a DC of 0.5, and an uninterrupted long lamellae design was used. This time, nickel was chosen as the material for comparison.

The grating was prepared exactly as the laser written samples. The second layer was afterward irradiated using x-ray irradiation and developed via the standard x-ray LIGA process. The following fabrication steps are based on a patent.[21] The grating is first bent to the desired radius with a polymer holder for electroplating. After electroplating, the grating is moved first into a metal separation clamp that stabilizes the radius of curvature by the principle of a 4-point bending. The polymer holder is now replaced by a final metal holder that allows the grating to be stripped (see Fig. 19).

Unfortunately, the grating already had a crack during production that was, after retrospective re-investigation, already present and visible in the flat grating. As a result of this, the grating developed only partially connected roof bridges in areas around the defective parts. In all other areas, the roof bridges were fully developed and of the same quality in a bent state as previously in the flat state (see Fig. 20). Ultimately, this defect led to the grating breaking during the holder exchange. Nevertheless, the resist was removed to demonstrate the feasibility of the method. SEM pictures, taken in the area without a defect, demonstrate the high quality of the structure. A radiography of the bent grating is presented in Fig. 21, where the grating is positioned at the distance from the source corresponding to the radius of curvature (12 cm). Leaving aside the defect caused by the breakage, the grating is of good quality; the expected horizontal profile is almost achieved.

6 Conclusion and Outlook

A solution was proposed to avoid the collapsing of the metallic lamellae when the resist must be removed; it consists of positioning perpendicular metal bridges on top of the grating (roof bridges). As metal, nickel was preferred to gold; the loss in transmission must be smaller than 5%. Different methods were tested; the most promising one is the structuring of a second resist layer applied onto a planarized grating. Furthermore, the fabrication of a grating in a curved state is demonstrated. To state the quality of the grating, the common SEM method is used.

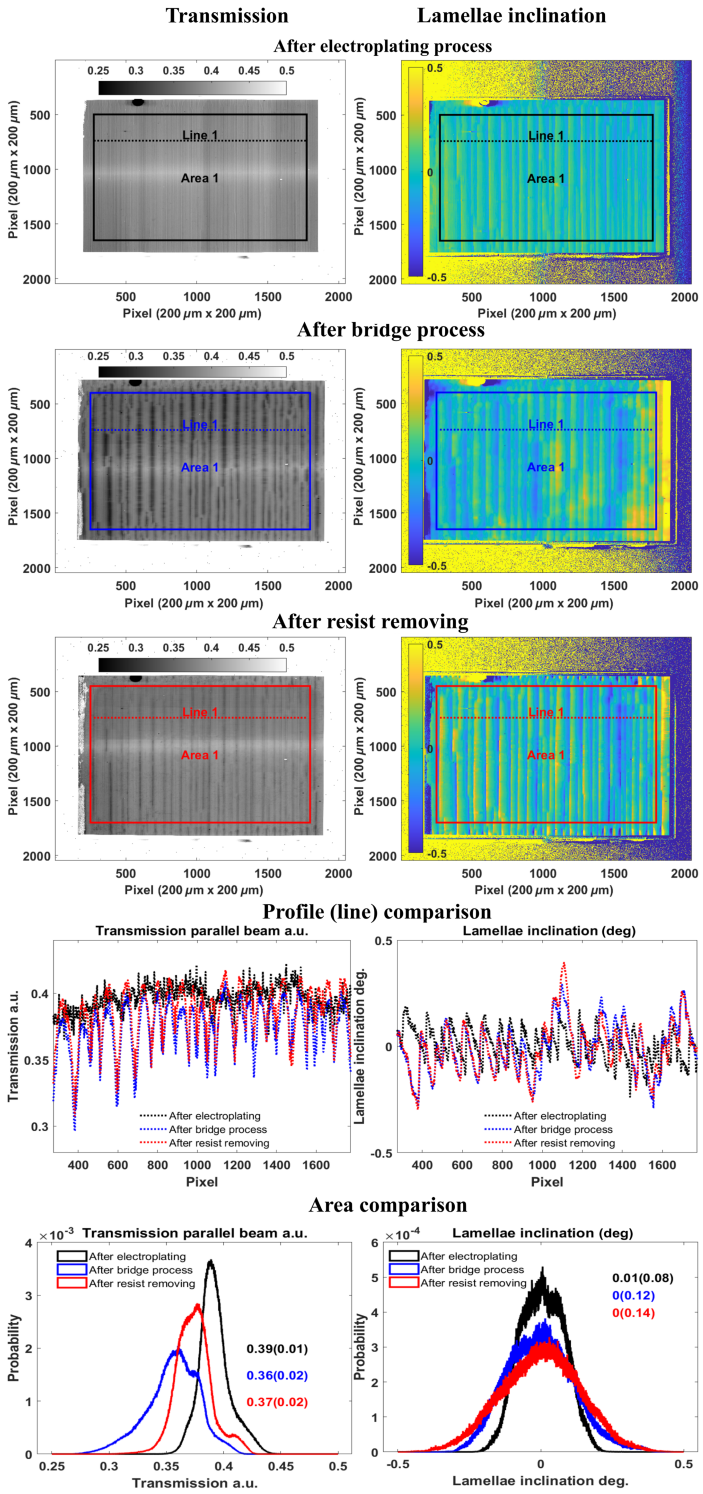

Fig. 17 Grating 1: AXT measurement results (transmission and lamellae inclination angle) before processing the roof bridges, after processing without removing the resist and after processing with removing the resist. An area and a profile are used for comparison.

To obtain more information, the AXT measurement technique is performed. The benefit to investigating the grating during the production step is substantial. The technique is recent and needs to be improved to arrive at a standard measurement method. Essentially this relates to, "Is the glass half empty or half full?" Grid stabilization works, but it is actually not 100% satisfactory. The overall quality is degraded; the planarization method tested here increases the defect (cracks) already present.

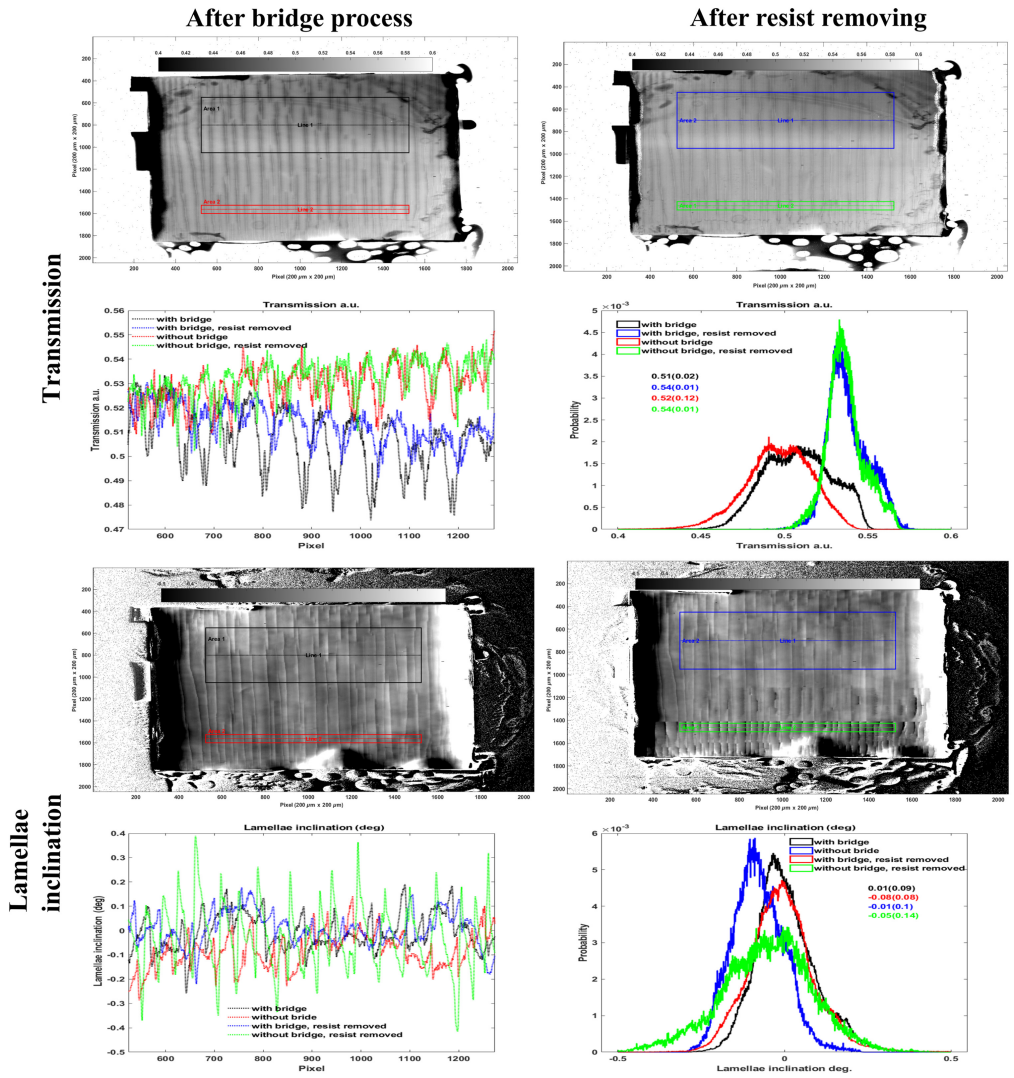

Fig. 18 Grating 2: AXT measurement results (transmission and lamellae inclination angle) after processing the roof bridges, without and with removing the resist. An area and a profile in a part of the grating with roof bridges and without roof bridges are used for comparison.

In conclusion, this publication addresses a critical challenge in the fabrication of metallic lamellae grating structures, particularly concerning the removal of the resist material. To prevent the undesirable collapsing of the metallic lamellae during resist removal, we proposed a unique solution involving the placement of perpendicular metal bridges on top of the grating, which we refer to as "roof bridges." In our investigation, we identified nickel as the preferred metal choice over gold, with the condition that the loss in transmission should be minimized to <5%. Our exploration involved the testing of various methods, and among these, the structuring of a second resist layer applied onto a planarized grating emerged as the most promising approach. In addition, we successfully demonstrated the fabrication of a grating in a curved state, expanding the potential applications of these structures.

To evaluate the quality of our gratings, we employed both conventional SEM and the more advanced AXT measurement technique. The latter provides valuable insights that complement SEM analysis. It is important to note that, although AXT measurements hold great promise, further refinement is necessary to establish it as a standardized measurement method in our field.

Addressing the age-old question of whether the glass is half-empty or half-full, our findings indicate that, although grid stabilization through roof bridges shows promise, it falls short of providing a perfect solution. The implementation of the planarization method tested here showed an unintended consequence of increasing defects, such as cracks, which were already present in

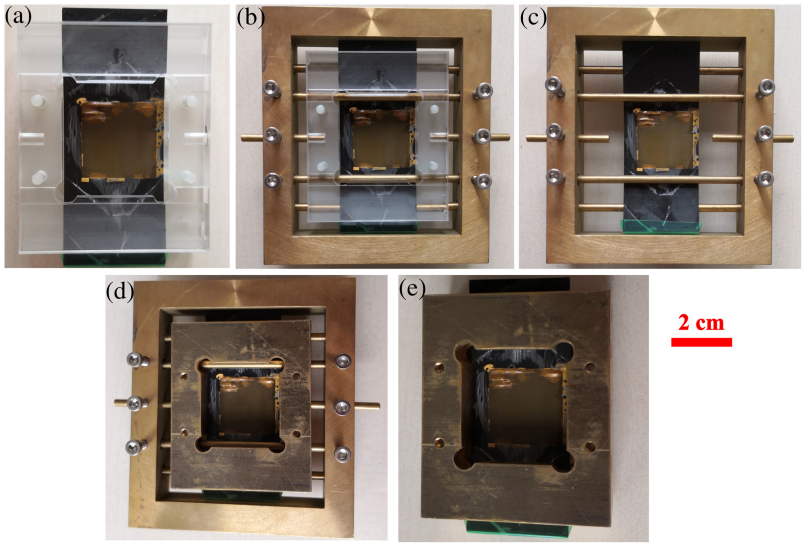

Fig. 19 (a) Bent grating in polymer holder after electroplating. (b) Bent grating with polymer holder in exchange clamp. (c) Bent grating stabilized solely in the exchange clamp. (d) Bent grating with final bending holder for stripping. (e) Final bent grating with roof bridges after the exchange clamp is removed. Note that the visible defect is a result of a thermal defect from an early grating production step.

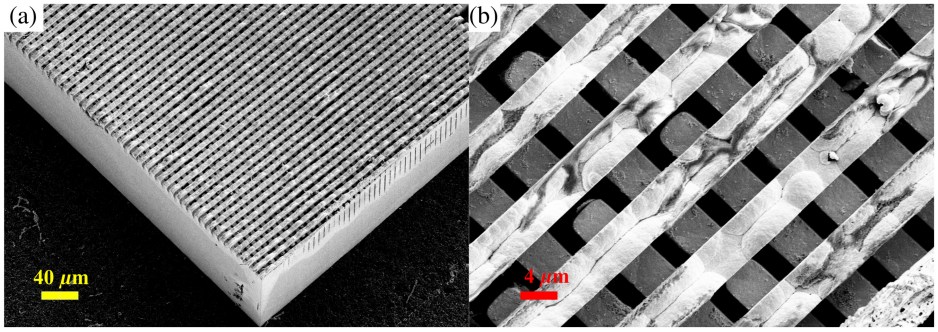

Fig. 20 The bent stabilized grating in the bending holder as measured in the SEM. (a) Fully stabilized area. (b) Close inspection of the well-defined Ni roof bridges in their bent state.

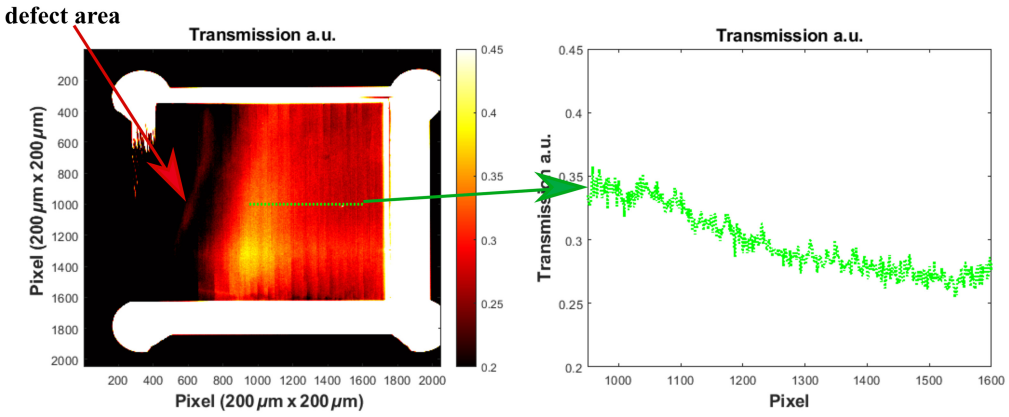

Fig. 21 Radiography of the grating in the bend holder. The grating is positioned at the distance from the source corresponding to the radius of curvature. The overall transmission and a profile are presented.

the gratings. In future work, alternative methods, such as lapping, will be explored and evaluated to improve the overall quality and integrity of these intricate structures.

In summary, our research has made significant strides in addressing the challenges associated with metallic lamellae grating fabrication. Although there is still work to be done in perfecting the measurement techniques and optimizing the fabrication processes, these findings represent valuable contributions to the field and pave the way for further advancements in this area.

Code and Data Availability

The data and code presented in this study is available from the corresponding author upon reasonable request.

Acknowledgments

The authors acknowledge the support of the Karlsruhe Nano Micro Facility (KNMFi) and the KARA Synchrotron light source facility at the Karlsruhe Institute of Technology (KIT), as well as funding from IT Health. The authors further acknowledge the support of the Karlsruhe School of Optics and Photonics (KSOP, financed by the Ministry of Science, Research and Arts of Baden-Württemberg as part of the sustainability financing of the projects of the Excellence Initiative II) and the KIT-Publication Fund of the KIT.

References

1. A. Momose, "X-ray phase imaging reaching clinical uses," *Phys. Med.* **79**, 93–102 (2020).
2. A. Momose et al., "Demonstration of x-ray Talbot interferometry," *Jpn. J. Appl. Phys.* **42**, L866 (2003).
3. C. Arboleda et al., "Towards clinical grating-interferometry mammography," *Eur. Radiol.* **30**, 1419–1425 (2020).
4. M. Viermetz et al., "Dark-field computed tomography reaches the human scale," *PNAS* **119**(8), e2118799119 (2021).
5. K. Willer et al., "X-ray dark-field chest imaging for detection and quantification of emphysema in patients with chronic obstructive pulmonary disease: a diagnostic accuracy study," *Lancet Digit. Health* **3**, e733–e744 (2023).
6. E. W. Becker et al., "Production of separation-nozzle systems for uranium enrichment by a combination of x-ray lithography and galvanoplastics," *Naturwissenschaften* **69**, 520–5232 (1982).
7. E. Becker et al., "Fabrication of microstructures with high aspect ratios and great structural heights by synchrotron radiation lithography, galvanoforming, and plastic moulding (LIGA process)," *Microelectron. Eng.* **4**(1), 35–56 (1986).
8. P. Meyer and J. Schulz, "Chapter 16: Deep x-ray lithography," in *Micromanufacturing Engineering and Technology*, Y. Qin, Ed., Micro and Nano Technologies, 2nd ed., pp. 365–391, William Andrew Publishing, Boston (2015).
9. K. Jefimovs et al., "High-aspect ratio silicon structures by displacement Talbot lithography and Bosch etching," *Proc. SPIE* **10146**, 101460L (2017).
10. L. Romano and M. Stampanoni, "Microfabrication of x-ray optics by metal assisted chemical etching: a review," *Micromachines* **11**(6), 589 (2020).
11. M. Richter et al., "Investigation on the mechanical interface stability of curved high aspect ratio x-ray gratings made by deep x-ray lithography," *J. Micro/Nanopattern. Mater. Metrol.* **21**(2), 024901 (2022).
12. A. del Campo and C. Greiner, "Su-8: a photoresist for high-aspect-ratio and 3D submicron lithography," *J. Micromech. Microeng.* **17**, R81 (2007).
13. F. Ceyssens and R. Puers, *SU-8 Photoresist*, pp. 2530–2543, Springer Netherlands, Dordrecht (2012).
14. B. Trimborn et al., "Imaging properties of high aspect ratio absorption gratings for use in preclinical x-ray grating interferometry," *Phys. Med. Biol.* **61**, 527–541 (2015).
15. N. Gustschin et al., "Quality and parameter control of x-ray absorption gratings by angular x-ray transmission," *Opt. Express* **27**, 15943–15955 (2019).
16. M. Schüttler et al., "Height control for small periodic structures using x-ray radiography," *Meas. Sci. Technol.* **27**, 025015 (2016).
17. J. Baró et al., "Penelope: an algorithm for Monte Carlo simulation of the penetration and energy loss of electrons and positrons in matter," *Nucl. Instrum. Methods Phys. Res. Sect. B Beam Interactions Mater. Atoms* **100**(1), 31–46 (1995).

18. Nuclear Energy Agency, *PENELOPE 2018: A Code System for Monte Carlo Simulation of Electron and Photon Transport*, p. 420 (2019).
19. E. Brinksmeier, *Diamond Machining*, pp. 1–6, Springer Berlin Heidelberg, Berlin, Heidelberg (2018).
20. M. Roeder, T. Guenther, and A. Zimmermann, "Review on fabrication technologies for optical mold inserts," *Micromachines* **10**(4), 233 (2019).
21. T. Koehler et al., "Stable top-bridge manufacturing for DAX gratings," US Patent App. 17/637,988 (2022).

Biographies of the authors are not available.